Dysregulation of Neuroprotective Lipoxin Pathway in Astrocytes in Response to Cytokines and Ocular Hypertension

Authors: Shruthi Karnam[1], Shubham Maurya[1], Elainna Ng, Amodini Choudhary[1], Arzin Thobani[1], John G Flanagan[1]*, Karsten Gronert[1,2]*

1. Herbert Wertheim School of Optometry and Vision Science, University of California Berkeley, Berkeley, California, United States.

2. Infectious Disease and Immunity Program, Herbert Wertheim School of Optometry and Vision Science, University of California Berkeley, CA, United States

Financial Support: This work was partly supported by the NIH grants R01EY030218 (KG, JGF) and P30EY003176.

Conflict of Interest: No conflicting relationship exists for any author.

Running head: Dysregulation of Neuroprotective Lipoxin Pathway in Astrocytes

***Corresponding Authors:**

*Karsten Gronert, Herbert Wertheim School of Optometry and Vision Science, Minor Hall, University of California Berkeley, Berkeley, CA 94720, USA. Email: kgronert@berkeley.edu

*John Flanagan, Herbert Wertheim School of Optometry and Vision Science, Minor Hall, University of California Berkeley, Berkeley, CA 94720, USA. Email: jgflanagan@berkeley.edu

Keywords: Glaucoma, astrocyte reactivity, lipoxygenase, neurodegeneration, retina, optic nerve

Abbreviations: LXB_4- Lipoxin B_4, LXA_4- Lipoxin A_4, IOP- Intraocular pressure, RGCs- Retinal ganglion cells, LOX- Lipoxygenase, ERG- Electroretinogram, OCT- Optical coherence tomography.

Abstract

Purpose: Glaucoma leads to vision loss due to retinal ganglion cell death. Astrocyte reactivity contributes to its neurodegeneration. Our recent study found that lipoxin B_4 (LXB_4), produced by retinal astrocytes, has direct neuroprotective actions on retinal ganglion cells. However, regulation of lipoxin formation and cellular targets for their neuroprotective activity in glaucoma remain to be defined. We investigated if ocular hypertension and inflammatory cytokines regulate astrocyte lipoxin pathway and if LXB_4 can regulate astrocyte reactivity.

Design: Experimental study.

Subjects/Participants/Controls: C57BL/6J mice were administered silicon oil into the anterior chamber to induce ocular hypertension (n=40). Age and gender-matched mice served as control subjects (n=40).

Methods: RNAscope in-situ hybridization, RNA-seq, and qPCR to analyze gene expression. LC/MS/MS lipidomics to assess functional expression of the lipoxin pathway. Retinal flat mounts and immunohistochemistry (IHC) to assess macroglia reactivity. OCT quantified the retinal layer thickness *in vivo,* and ERG assessed retinal function. Primary human brain astrocytes were used for *in vitro* reactivity experiments. Non-human primate optic nerves were used to assess gene and functional expression of the lipoxin pathway.

Main Outcome Measures: Intraocular pressure, RGC function, OCT measurements**,** gene expression, in situ hybridization, lipidomic analysis, and IHC.

Results: Gene expression and lipidomic analysis established functional expression of the lipoxin pathway in the mouse retina, optic nerve of mice and primates, as well as human brain astrocytes. Ocular hypertension caused significant dysregulation of this pathway, with an increase in 5-lipoxygenase (5-LOX) activity and a decrease in 15-lipoxygenase activity. This

dysregulation was coincident with a marked upregulation of astrocyte reactivity in the mouse retina. Reactive human brain astrocytes also showed a marked increase in 5-LOX. Administration of LXB_4 regulated the lipoxin pathway, restored and amplified LXA_4 generation, and mitigated astrocyte reactivity in mouse retinas and human brain astrocytes.

Conclusions: The lipoxin pathway is functionally expressed in retina and brain astrocytes, optic nerves of rodents and primates, a resident neuroprotective pathway that is downregulated in reactive astrocytes. Novel cellular targets for LXB_4's neuroprotective action is inhibition of astrocyte reactivity and restoration of lipoxin generation. Amplifying the lipoxin pathway is a potential target to disrupt or prevent astrocyte reactivity in neurodegenerative diseases.

Introduction

Glaucoma is a neurodegenerative disease that is responsible for irreversible blindness globally. The condition is characterized by degeneration of retinal ganglion cells (RGCs) and their axons [1,2]. Unfortunately, it is estimated that the number of people affected by glaucoma will increase to 112 million worldwide by 2040 [3]. Although intraocular pressure (IOP) is the only modifiable risk factor, nearly 50% of patients suffer from glaucomatous damage even after lowering IOP [4]. Recent studies have shown that the damage caused by glaucoma is not only limited to the RGCs and axons but also extends to the brain [5]. There is an unresolved need to develop neuroprotective strategies to prevent or delay the death of RGCs, independent of IOP, in glaucoma [6].

Lipoxins (LXA_4 and LXB_4) are eicosanoids generated from arachidonic acid. Their canonical protective actions in various pathological processes include regulating the initial response of innate and adaptive immune cells and promoting the resolution of acute inflammation [7-9]. We recently identified a non-canonical protective action of lipoxins, namely

their direct regulation of RGCs [10]. The human and mouse receptor for LXA_4, formyl peptide receptor 2 (FPR2/ALX) [11], is expressed in RGCs. A receptor for LXB_4, the lipoxin with more potent neuroprotective actions in the retina [10], has yet to be identified. The biosynthesis of lipoxins requires the coordinated interaction of 5-lipoxygenase (LOX) with 12/15-LOX enzymes [12,13] . Primary astrocytes generate lipoxins *in vitro* and acute exocytotoxic stress downregulates lipoxin formation and lipoxygenase expression in the retina. However, the regulation of the lipoxin pathway in ocular hypertension has yet to be investigated. More importantly, it is unclear if retinal astrocyte reactivity, a primary response to ocular hypertension, regulates the astrocyte lipoxin pathway and whether lipoxin formation is a unique phenotype of mouse retinal astrocytes. These knowledge gaps are of interest as therapeutic amplification of the retinal lipoxin pathway is a potential neuroprotective target.

Astrocytes are glial cells in the central nervous system and retina and play a crucial role in maintaining homeostasis. They provide metabolic substrates, growth factors, and trophic support to neurons and are also involved in synapse formation and plasticity [14]. Astrocytes also work closely with the immune system, as they can detect danger signals, respond to secreted cytokines and chemokines, and activate adaptive immune responses [15]. In glaucoma, astrocytes in the optic nerve head and retinal nerve fiber layer are particularly vulnerable to mechanical and ischemic insult caused by elevated IOP, which leads to reactive gliosis. Reactive astrocytes release pro-inflammatory molecules and oxidative stress-inducing factors, which can cause neuroinflammation and neuronal damage [16]. Recently, it has been suggested that microglial release of pro-inflammatory cytokines can induce the formation of neurotoxic reactive astrocytes in the retina and brain [17]. Limited studies have investigated potential therapeutic strategies to prevent or reverse astrocyte reactivity in neurodegenerative diseases.

In this study, we aimed to investigate the regulation and functional expression of lipoxin pathways in the mouse retina, optic nerve of mice and primates, and human astrocytes. We also examined if the neuroprotective action of the autacoid LXB_4 includes reducing astrocyte reactivity in response to inflammatory cytokine-induced activation and ocular hypertension.

Materials and Methods

Mice

C57BL/6J male mice (Jackson Laboratory, Bar Harbor, ME) were allowed to acclimatize to the housing facility for 2 wks before experimentation. Mice studies were performed in compliance with the ARVO Statement for the Use of Animals in Ophthalmic and Vision Research, and all experimental procedures were approved by the Institutional Animal Care and Use Committee (IACUC) at the University of California, Berkeley. Mice used in this study were maintained in a pathogen-free vivarium under a 12-hour dark and light cycle with *ad libitum* food and water.

Induction of ocular hypertension by injection of silicon oil

Ocular hypertension was induced in the 8 wk old C57BL/6J mice by injection of 1.2 μL of pharmaceutical-grade silicon oil (Alcon silikon 1000, Geneva, Switzerland) in the anterior chamber of both eyes, as published previously by Jie Zhang and colleagues [18-20]. Briefly, 8 wk old mice were anesthetized by an intraperitoneal injection of ketamine/xylazine (100mg/kg and 10mg/kg, respectively). One drop of topical anesthetic (proparacaine hydrochloride, 0.5%, Akorn, Lake Forest, IL) was applied to the cornea of both eyes before the injection. 1.2 μL of silicon oil was injected into the anterior chamber of both eyes through a 30 G Hamilton glass syringe. After injection, a drop of antibiotic (Tobramycin Ophthalmic Solution 0.3%) was placed

on the eye. Sterile PBS (phosphate-buffered saline) was injected into another set of mice and used as a control. Mice were euthanized at 2, 4, and 8-wk time points following injections for various experimental procedures.

IOP Measurements/Pupil Dilation

IOP was monitored once every 2 wks until 8 wks after silicon oil injection using TonoLab tonometer (Colonial Medical Supply, Londonderry, NH). Since IOP measurement requires pupil dilation, each IOP measurement can be considered a pupil dilation treatment. Pupil dilation was achieved according to the published protocol [18-20].

Cell Culture

Cultured primary human cortical astrocytes (HA1800) were purchased from ScienCell (Carlsbad, CA) and treated with cytokines: IL-1α, TNF- α, and C1q for 24 hrs [21]. Astrocytes were treated with LXB_4 (Cayman Chemicals, Ann Arbor, MI) (1μM) or vehicle for 20 mins before adding cytokines. After 24 hrs, the cells were collected in Trizol (Invitrogen, Waltham, MA) for RNA isolation or ice-cold methanol for lipidomic analysis. For primary retinal astrocytes, four mice retinas were pooled and digested using papain (Worthington, Lakewood, NJ) and plated on Poly-D-Lysine coated flasks with Astrocyte Growth Media (Lonza, Basel, Switzerland), changing the media every 3 days.

Bulk RNA-seq

Total RNA from Macaque optic nerves (n=2) were extracted using Trizol extraction. Sequencing libraries were prepared using SMARTer v4 Ultra Low Input RNA Kit (Clontech, Mountain View,

CA). Sequencing was performed on Novaseq S4 150PE platform (Illumina, San Diego, CA). Library preparation and RNA-seq were performed at the QB3 Genomics, UC Berkeley, Berkeley, CA, RRID: SCR_022170. Quality check of FASTQ files was performed with FastQC v.0.11.9, and adapters sequences were trimmed using Trim Galore! v.0.6.6. Trimmed reads were mapped on mouse genome version mm39 (University of California Santa Cruz) with STAR alignment tool v.2.7.1a using RefGene annotation. The total number of read counts mapped for each gene was extracted from BAM files using FeatureCount v.1.5.3. Count matrix was imported into Rstudio v.4.2.0. It was normalized using the Transcripts Per Million method by NormalizeTPM. Mean values of normalized counts for each gene were plotted for visualization.

Electroretinography

Before measuring the ERG, the mice underwent overnight dark adaptation. They were then anesthetized and received Tropicamide (1%, Akorn, Lake Forest, IL) and phenylephrine (2.5%, Paragon BioTeck, Portland, OR) to dilate their pupils. The Celeris system (Diagnosys LLC, Lowell, MA) was used to conduct the ERG measurement, with stimulus intensities ranging from -5.90 to 2.25 log cd.s/m^2. The tail subdermal needle electrode served as ground. A positive scotopic threshold response (pSTR) elicited with the intensity of -2.50 log cd.s/m^2 was used to represent the RGC function (average of 20 repeats, inter-stimulus interval of 2 seconds).

Optical Coherence Tomography

Before imaging, mice received anesthesia and were given lubricant eye drops. We used a Bioptigen spectral domain OCT system (Envisu R2300, Durham, NC) for imaging. Our previous studies described the OCT image acquisition and analysis protocols [22,23]. We captured an en-face

retinal fundus image with the optic nerve head in the center, using a 1.8 x 1.8 mm rectangular scanning. Each replication involved 100 B-scan images (1536 A-scans for each B-scan). Retinal layer B-scan images were analyzed by masked observers using Image J software. We quantified the thickness of the retinal layer at left and right locations from the center of the optic nerve head in each retinal quadrant. The average data from both locations represented the thickness value.

Retinal Flat Mount and RGC Quantification

Eyes were removed at 8 wks and fixed with 4% paraformaldehyde (PFA). Posterior eyecups were incubated overnight in the blocking buffer (10% normal donkey serum and 2% PBS-Triton-X-100). Eyecups were stained with primary antibodies, GFAP (Abcam, Cambridge, UK), and RBPMS (Phosphosolutions, Aurora, CO) (1:1000 dilution each) and were incubated on a shaker for 48-72 hrs at 4 ^{o}C. After incubation, eyecups were washed with 0.25% PBST and incubated with either Alexa fluor 488 or 594 conjugated secondary antibodies (Invitrogen; at 1:1000 dilution) under dark conditions for 2 hrs at room temperature. After washing with PBST, the retinas were gently detached, and four perpendicular clover cuts were made. ProLong™ Gold Antifade Mountant (#P36930, Invitrogen, Eugene, OR) was added to mount the retinas. Retinas were imaged on a Nikon Ti Eclipse microscope using a 20x objective. A minimum of 5-6 independent specimens (biological replicates) were analyzed for each flat mount.

Immunohistochemistry

The eyes were fixed in 4% PFA and transferred into 30% sucrose. Tissues were then embedded in OCT media and cut into 10-µm-thick sections using a CM1900 Cryostat (Leica, Wetzlar, Germany). Primary human astrocytes were fixed with 4% PFA for 20 mins. Then cells were

permeabilized with 0.3% Triton®-X-100 PBS for 5 mins at room temperature. Sections and cells were blocked using a blocking buffer (5% donkey serum in 0.3% Triton X-100 containing PBS) for 30 mins. Primary antibodies GFAP (Abcam), RBPMS (Phosphosolutions), LCN2 (Invitrogen), 5-LOX (Abcam), Pax2 (Abcam), Vimentin (Invitrogen), and CD44 (Proteintech) were added in blocking buffer and incubated overnight at 4 °C. Sections, and cells were washed and incubated with Alexa fluor 488 and 594 conjugated secondary antibodies (Invitrogen; at 1:1000 dilution) for double labeling for 2 hrs at room temperature under dark conditions. They were then washed and mounted using ProLong™ Gold Antifade Mountant, and images were captured using a Nikon Ti Eclipse microscope.

RNAscope in situ hybridization

RNA in situ hybridization for *Alox5*, *Alox15*, and *Fpr2* mRNA was performed manually using RNAscope Multiplex Fluorescent Reagent Kit v2 Assay (Advanced Cell Diagnostics, Inc., Newark, CA) according to the manufacturer's instructions. Images were acquired on a Nikon Ti Eclipse microscope using a 40× objective. RNAscope probes used were as follows: *Alox15* (Cat. No: 539781-C1), *Alox5* (Cat. No: 436101-C2), and *Fpr2* (Cat. No: 509281-C3).

qPCR

RNA was isolated from mouse retinal tissue and human brain astrocytes and quantified according to our published protocol [10]. *Gapdh* was used as the reference gene. Mouse primers used in this study are listed in Table. Primers for the human genes used in this study are listed in Table 2 (please refer to supplementary material for primer details).

LC-MS/MS

Retinas were immediately snapped, frozen on dry ice, and stored at −80°C before processing for lipidomic analyses. Eicosanoids and PUFA in the cells and conditioned media from astrocyte cultures were identified and quantified by LC-MS/MS according to our published protocol [10].

Statistical Analysis

All values are presented as mean ± standard error of the mean (SEM) of n observations, where n represents the number of animals studied or independent *in vitro* experiments. Statistical analysis was performed using GraphPad Prism 9.0 (GraphPad Software, San Diego, CA). One-way ANOVA followed by post hoc Tukey's multiple comparison test or unpaired Student's t-test was used to compare intergroup differences. Comparing results were considered statistically significant when $P<0.05$.

Results

Lipoxin pathway is expressed in mouse retina, optic nerve, and retinal astrocytes.

The expression of lipoxin pathways was investigated in the retina, optic nerve, and retinal astrocytes of C57BL/6J mice. RNAscope in situ hybridization was performed on the retina and myelinated optic nerve region cross-sections to determine the cell-specific expression of *Alox5, Alox15, and Fpr2*. The data showed that the lipoxin circuits were localized in the Ganglion cell layer (GCL), inner nuclear layer (INL), and outer nuclear layer (ONL) of the retina, and in the optic nerve region (Fig. 1A). To confirm expression of the lipoxin circuits in retinal astrocytes, qRT-PCR was performed on cultured primary mouse retinal astrocytes. The results showed that *Alox5, Alox15, and Fpr2* were expressed with average Ct values of 28.23±0.3, 29.07±0.3, and

28.58±0.2, respectively. Notably, higher RNA expression was observed in the optic nerves with average Ct values of 27.75±0.2 (Alox5), 24.65±0.6 (Alox15), and 25.94±0.7 (Fpr2) (Fig. 1B). These results confirm expression of the lipoxin pathway in the retina and optic nerve of mice, including retinal astrocytes.

Lipoxin pathway is expressed in macaque optic nerves and human primary brain astrocytes

To explore expression of the lipoxin pathway in primates, we conducted RNA-seq analyses on macaque optic nerves. Results established high expression of *ALOX15*, moderate expression of *ALOX5* and *ALOX5AP*, and lower expression of *ALOX12, ALOX15B, FPR2,* and *FPR3* genes (Fig. 2A). Lipidomic analysis confirmed active eicosanoid pathways and lipoxin formation in primate optic nerves as evidenced by the presence of released arachidonic acid and significant levels of 5-HETE, 12-HETE, 15-HETE and LXB_4 (Fig. 2B). The cell identity of the primary human brain astrocytes line was validated by positive staining with astrocyte-specific markers GFAP, Vimentin, Pax2, and CD44 (Fig. 2C). Primary human astrocytes, like primate optic nerves, also expressed the lipoxin pathway, namely *ALOX5, ALOX15,* and *FPR2*, and lipidomic analyses confirmed endogenous formation of eicosanoids and lipoxins. Interestingly, cultured human brain astrocytes generated both LXA_4 and LXB_4 (Fig. 2D). These data demonstrate that neuroprotective lipoxins are formed by retina, optic nerve, and brain and are present in murine and primate species, including humans.

Validation of the mild chronic model of ocular hypertension

IOP and RGC density changes were assessed in control and silicon oil-injected eyes of mice. Fig. 3A shows that IOP was significantly elevated in the silicon-injected eyes compared to control eyes. After 8 wks, mice were euthanized, and RGC density was assessed by staining flat-mounted retinas with RGC marker, RBPMS (Fig. 3B). Peripheral RGC loss of 17% was observed in silicon oil-injected eyes compared to control eyes (Fig. 3C). Changes in RGC function were measured longitudinally using ERG measurements of pSTR. The average waveforms of pSTR elicited by a flash intensity of -2.5 log cd.s/m^2 at 8 wks (Fig. 3D). The results indicated a loss of RGC function in hypertensive eyes compared to control normotensive eyes. Additionally, loss in ganglion cell complex (GCC) thickness, a clinically relevant biomarker of nerve fiber loss, was measured longitudinally by OCT (Fig. 3E). Mild ocular hypertension caused a significant 10% relative loss ($p<0.05$) compared to normotensive control eyes (Fig. 3F). Overall, these results confirm that the silicon oil model of mild chronic ocular hypertension maintains a stable and elevated IOP that leads to morphological and functional RGCs loss and is a well-suited model to investigate the slow onset of glaucomatous-like pathogenesis.

Dysregulation of lipoxin pathway in response to chronic mild ocular hypertension

Lipoxin pathway gene expression was analyzed in retinas from normotensive and hypertensive eyes at 2, 4, and 8 wks to investigate regulation of lipoxin pathway in response to chronic mild ocular hypertension. Results demonstrate that *Alox5AP* (5-lipoxygenase activating protein, FLAP), which is a cofactor required for full 5-LOX enzymatic activity, was significantly upregulated at 2 and 4 wks, while there was no change in the levels of *Alox5* in response to

ocular hypertension. Interestingly, the levels of *Alox15* and *Fpr2* were significantly upregulated initially at 2 and 4 wks but significantly downregulated at 8 wks (Fig. 4A). To investigate the functional dysregulation of the lipoxin pathway; four retinas were pooled at 4 wks and analyzed by LC/MS/MS-based lipidomics to establish formation and changes in eicosanoid and PUFA profiles. Lipidomic analysis demonstrated that arachidonic acid (AA) and the 15-LOX pathway marker, 15-HETE, were significantly decreased in response to ocular hypertension. In contrast, the 5-LOX pathway markers, 5-HETE, and 4-HDHA were significantly increased (Fig. 4B). These findings indicate that expression of the homeostatic lipoxin pathway is dynamically regulated during ocular hypertension and that activity of 5-LOX and 15-LOX is dysregulated.

Activation of Müller glia and astrocyte reactivity markers in response to ocular hypertension

The impact of mild ocular hypertension on astrocyte and Müller glial reactivity was assessed by immunofluorescent staining of retinal cross-sections with cell-specific reactivity markers from normotensive and hypertensive eyes. Expression of GFAP, an intermediate filament protein that is a marker of macroglial reactivity, was induced and upregulated in Müller glia and astrocytes, as early as 2 wks after ocular hypertension (Fig. 5A), and remained upregulated in the retina for 8 wks and was coincident with loss of RGCs as evidenced by RBPMS staining in the GCL layer (Fig. 5B). GFAP staining of retinal flat mounts also established marked reactive astrogliosis after 8 wks of mild ocular hypertension (Fig. 5C). To investigate macroglia reactivity further, we measured glutamate aspartate transporter (GLAST) gene expression, which is highly expressed in Müller cells as part of their homeostatic function to support RGCs. GLAST expression was significantly decreased after 2 and 4 wks of ocular hypertension (Fig. 5D). Gene expression of

signature astrocyte reactivity markers (*Gfap, Lcn2, Steap4, Gbp2, Serping1, and Fbln5*) were significantly upregulated in response to ocular hypertension at 2, 4, and 8 wks compared to normotensive controls (Fig. 5E). These results establish that Müller glia and astrocyte reactivity is a key and early feature of mild ocular hypertension.

Therapeutic LXB_4 treatment reduces astrocyte and Muller glia reactivity in the mouse retina

We next assessed if the neuroprotective actions of lipoxins in ocular hypertension [10] include regulation of macroglia reactivity. Therapeutic LXB_4 methyl ester treatment (n=8, 5ng/g IP; 0.5ng/g topical) was initiated after 1 wk of ocular hypertension and administered every other day until the 4th wk. The dosing and preparation of lipoxins were based on previous studies [10,24]. qPCR analysis of macroglia reactivity markers established that treatment with LXB_4 resulted in a significant up-regulation of GLAST. In addition, LXB_4 treatment significantly downregulated astrocyte reactivity markers such as *Lcn2* and *Steap4*. The levels of *Gbp2, Serping1, and Fbln5* remain unchanged (Fig. 6). These findings identify a potentially novel mechanism for the neuroprotective actions of LXB_4 treatment, namely reversing macroglia reactivity and restoring their homeostatic function.

LXB_4 treatment modulates the lipoxin pathway in primary human brain astrocytes

To establish macroglia-specific actions for LXB_4, we used primary human brain astrocytes which express a fully functional lipoxin pathway identical to that found in the mouse primary retinal astrocytes (Fig. 2D). To induce astrocyte reactivity, cells were treated with established inflammatory cytokines, which are also generated in the retina in response to ocular hypertension

[21]. qPCR analysis confirmed that cytokine treatment significantly upregulated reactive astrocyte markers, including *LCN2*, *SERPING1*, and *C3*, in primary human brain astrocytes. LXB_4 treatment significantly downregulated these astrocyte reactivity markers (Fig. 7A). Immunofluorescence analysis of LCN2 was consistent with the qPCR findings. These results establish direct regulation of astrocyte reactivity as a new bioaction of LXB_4.

Reactive astrocytes also showed increased gene expression of 5-LOX (ALOX5) compared to controls. LXB_4 treatment reduced 5-LOX expression in reactive astrocytes (Figs. 7A and B). Hence, we examined the functional consequence of LXB_4 regulation of 5-LOX expression in reactive astrocytes. Consistent with changes in 5-LOX gene expression (Fig 7B), 5-HETE formation was significantly increased in reactive astrocytes, and LXB_4 treatment reduced 5-HETE generation. More importantly, reactive astrocytes generated less LXA_4, but LXB_4 treatment restored and amplified LXA_4 formation in reactive astrocytes (Fig. 7C). Concentrations of added LXB_4 in media remained high after 24 hrs, so we were unable to assess if LXB_4 treatment also amplified endogenous astrocyte LXB_4 formation. These findings suggest LXB_4 restores the homeostatic phenotype and recovers and amplifies neuroprotective lipoxin formation in cytokine-challenged primary human astrocytes.

Discussion

Glaucoma results in the gradual loss of retinal ganglion cells (RGCs), leading to irreversible vision loss [25]. Astrocyte reactivity is a key pathological mechanism that contributes to the neurodegeneration of RGCs in glaucoma, as they play a crucial role in maintaining the health and function of RGCs [26]. Recently, we identified that lipoxins (LXA_4 and LXB_4) derived from astrocytes promote neuroprotection against acute and chronic injury in the retina by directly

acting on RGCs [10]. However, the regulation of lipoxin formation in the retina and the extent of their neuroprotective activity in glaucoma remains to be defined.

Our study revealed that astrocytes express 5-LOX and 15-LOX, two enzymes essential for lipoxin generation by a single cell[12,13,27]. We assessed the functional activity of the lipoxin pathway through LC/MS and confirmed the presence of endogenous lipoxin formation and activity of 5-LOX and 15-LOX in rodent and primate astrocytes, retina, and optic nerves. Notably, we observed lipoxin formation in the optic nerves of non-human primates, which, to our knowledge, has not been previously reported. Additionally, we demonstrated formation of both LXA_4 and LXB_4 by primary human brain astrocytes, aligning with a recent study reporting lipoxin formation in astrocytes of human brain organoids using ELISA [28]. Astrocytes, the most abundant cell type in the central nervous system, play a vital regulatory role in neurogenesis, synaptogenesis, blood-brain barrier permeability, and extracellular homeostasis, impacting various aspects of brain function [29]. These results emphasize the potential significance of the resident neuroprotective lipoxin pathway not only in the retina but also in the brain and optic nerve [10,30].

5-LOX is required to generate leukotrienes, which are pro-inflammatory lipid mediators, and this enzyme has been implicated in promoting pro-inflammatory lipid mediator synthesis in various neurodegenerative diseases [31]. However, 5-LOX is also required for generating lipoxins and most of the pro-resolving lipid mediators (SPM) [9,12,30]. Hence, the role of 5-LOX is context and cell dependent. In the retina, 5-LOX has been identified as the essential enzyme for the protective actions of dietary DHA supplementation in retinopathy of prematurity [32]. Moreover, in 5-LOX knockout mice, autoimmune uveitis pathogenesis is markedly amplified, and in a retinal model

of glutamate exocytotoxic, 5-LOX inhibition amplifies retinal ganglion cell death [10]. These findings indicate that in the retina, homeostatic 5-LOX has protective functions.

The function of 5-LOX, namely the products this pathway generates, depends on the balanced interaction with 15-LOX, an interaction that leads to lipoxin formation. 15-LOX is highly expressed in epithelial cells of healthy mucosal tissues, retinal pigmented epithelial cells, tissue-resident homeostatic macrophages, immune regulatory macrophages and polymorphonuclear leukocytes (PMN) [33-36]. 15-LOX has immunoregulatory and wound healing roles important for maintaining tissue homeostasis, especially in the eye [33-35,37]. A key feature of an immune-regulatory and pro-resolving phenotype of PMN is high expression of 15-LOX to enable generation of lipoxins[34,38]. Dysregulation of the balanced expression and function of 5- and 15-lipoxygenases has been implicated in several neurodegenerative diseases [30] and deletion of either 5-LOX or 15-LOX amplifies experimental allergic encephalomyelitis in mice [39]. Our findings reveal a shift in the homeostatic balance of 5-LOX and 15-LOX activities in the retina and astrocytes as a feature of reactivity and ocular hypertension induced pathogenesis. Astrocyte reactivity and retinal response to ocular hypertension correlated with an increase in 5-LOX and a decrease in 15-LOX activity. Interestingly, our findings of dysregulated lipoxygenase activity are consistent with previous studies that have reported increased levels of 5-LOX activity in Alzheimer's disease (AD) [40-42]. Additionally, a separate study reported decreased levels of 15-LOX in the CA1 region of the hippocampus in patients with moderate to severe stages of AD [43]. In contrast, several studies have demonstrated that inhibition of mouse 12/15-LOX enzymes can reduce ischemic injury and diabetic pathogenesis [44,45]. In short, there is a complex interplay between 5- and 15- LOX, and their dynamic regulation and dysregulation is a key feature of neurodegenerative diseases such as Alzheimer’s and glaucoma.

Our study has identified a novel target for the neuroprotective effects of LXB_4, demonstrating its ability to inhibit astrocyte reactivity both *in vitro* and *in vivo*. Astrocytes play a crucial role in maintaining the health and function of RGCs and the vasculature in the retina and optic nerve. Astrocyte reactivity has been implicated as a key pathological feature in various neurodegenerative diseases, including glaucoma [46,47]. Our findings establish, for the first time, a direct action of LXB_4 on macroglia by downregulating key reactive markers in primary human astrocytes *in vitro*. This highlights the significance of LXB_4 as an autocrine signal in astrocytes, similar to its established role in PMN, the primary cell type that generates lipoxins, but also the primary cell target to downregulate their pro-inflammatory function during acute inflammation[12,34,48]. Thus, our results suggest that LXB_4 serves as an autocrine signal in astrocytes, downregulating their reactive phenotype.

Previous studies have demonstrated the anti-inflammatory effects of lipoxins in various neuroinflammatory diseases, indicating their therapeutic potential [7]. However, the source of lipoxins in the central nervous system and the potential targets for their protective actions have not been thoroughly investigated. Our study reveals that LXB_4 treatment restores and significantly amplifies the generation of LXA_4, another lipoxin with distinct bioactions, in reactive astrocytes. The specific receptor for LXB_4, distinct from the LXA_4 receptor Fpr2/ALX, remains to be identified, as does the mechanism underlying the upregulation of lipoxin formation in astrocytes. LXB_4 treatment reduced amplified 5-LOX activity in reactive human astrocytes, suggesting that restoring the balanced interaction between 5-LOX and 15-LOX may partly explain the restoration of lipoxin production in astrocytes.

Acknowledgments

This work was partly supported by the NIH grants R01EY030218 (KG, JGF) and P30EY003176.

Figure legends

Figure 1. Expression of lipoxin pathway in mouse retina and optic nerve. **(A)** Representative images of RNAscope ISH (red) (indicated with white arrows) of retina and optic nerve using mRNA probes for *Alox5*, *Alox15*, and *Fpr2*. Nuclei were labeled with DAPI to distinguish nuclear layers of the retina. All images were obtained using a 40X objective. Scale bar = 50 µm. Labels: ganglion cell layer (GCL), inner nuclear layer (INL), outer nuclear layer (ONL). **(B)** Bar graph represents Ct values of lipoxin pathway genes in retinal astrocytes and optic nerve analyzed by qPCR (n=3).

Figure 2. Expression of lipoxin pathway in optic nerve of primates and primary human brain astrocytes. **(A)** RNA-seq in macaque optic nerve showing lipoxin pathway genes (n=2). **(B)** LC/MS/MS-based lipidomic quantification of endogenous lipid mediators in primate optic nerve (n=2). **(C)** Representative immunofluorescence images of primary human brain astrocytes stained with GFAP, Pax2, Vimentin, and CD44. **(D)** LC/MS/MS-based lipidomic quantification of endogenous lipid mediators in human brain astrocytes (n=2).

Figure 3. Validation of the silicon oil model. **(A)** IOPs were increased after silicon oil (SO) injection (n=20). **(B)** Representative confocal images of flat-mounted retina sections showing surviving RBPMS-positive (red) RGCs at 8 wks. Scale bar = 50 µm. **(C)** Bar graph indicates % of mid-peripheral RGC loss. **(D)** Average ERG waveforms of RGC responses (pSTR, -2.5 log

cd.s.m^{-2}) at wk 8 for each group. **(E)** Representative OCT images of mouse retina at 8 wks. GCC: ganglion cell complex, including RNFL, GCL, and IPL layers, indicated by double-ended yellow arrows. **(F)** Bar graph indicating % reduction in GCC thickness at 8 wks. (n=4-6). ****p< 0.001. (Ctrl- Control; OHT- ocular hypertension).

Figure 4. Regulation of lipoxin pathway in response to ocular hypertension. **(A)** The time course response of lipoxin pathway genes was analyzed by qPCR at 2, 4, and 8 wks. The results were normalized to GAPDH and age-matched controls. n=3-4 (2 retinas were pooled for each replicate). **(B)** LC/MS/MS-based lipidomic quantification of endogenous lipid mediators in the mouse retina at 4 wks, n=3 (4 retinas were pooled for each replicate). *p< 0.05, **p<0.01, **p<0.001. (Ctrl- Control; OHT- ocular hypertension).

Figure 5. Regulation of astrocyte reactivity in response to ocular hypertension. **(A)** Representative immunofluorescence images of GFAP (green) at 2 wks, and **(B)** GFAP (green) RBPMS (red) at 8 wks of ocular hypertension. Nuclei were labeled with DAPI. All images were obtained using a 40× objective. Scale bar = 50 µm. Labels: ganglion cell layer (GCL), inner nuclear layer (INL), outer nuclear layer (ONL). **(C)** Representative images of a portion of flat-mounted retinas stained with GFAP (green) at 8 wks. **(D)** Muller glia reactivity gene, GLAST, analyzed by qPCR at 2 and 4 wks. The results were normalized to GAPDH. **(E)** Astrocyte markers were significantly upregulated at 2, 4, and 8 wks when analyzed by qPCR. Results were normalized to GAPDH and controls. n=4 (2 retinas were pooled for each replicate). *p< 0.05, **p<0.01, **p<0.001. (Ctrl- Control; OHT- ocular hypertension).

Figure 6. Effect of LXB_4 treatment on astrocyte reactivity markers in the mouse retina**.** LXB_4 methyl ester treatment (n=8, 5ng/g IP; 0.5ng/g topical) was started after one week of silicon injection every other day till the 4th week. Treatment of LXB_4 modulates astrocyte reactivity genes in the ocular hypertension model, n=4 (2 retinas were pooled for each replicate). (Ctrl-Control; OHT- ocular hypertension). *p< 0.05, **p<0.01, ***p<0.001.

Figure 7. Effect of LXB_4 treatment on lipoxin pathway in human brain astrocytes. **(A)** Astrocyte reactivity genes analyzed by qPCR. The results were normalized to GAPDH. Data is mean±SEM, n=3-4. **(B)** Representative immunofluorescence images of LCN2 and 5-LOX. Nuclei were labeled with DAPI. **(C)** LC/MS/MS-based lipidomic quantification of endogenous lipid mediators, n=4-5. (Ctrl-Untreated control astrocytes, RA- Reactive astrocytes). *p< 0.05, **p<0.01, ***p<0.001.

References

1. Nucci C, Martucci A, Giannini C, Morrone LA, Bagetta G, Mancino R. Neuroprotective agents in the management of glaucoma. *Eye (Lond)*. May 2018;32(5):938-945. doi:10.1038/s41433-018-0050-2
2. Tham YC, Li X, Wong TY, Quigley HA, Aung T, Cheng CY. Global prevalence of glaucoma and projections of glaucoma burden through 2040: a systematic review and meta-analysis. *Ophthalmology*. Nov 2014;121(11):2081-90. doi:10.1016/j.ophtha.2014.05.013
3. Jonas JB, Aung T, Bourne RR, Bron AM, Ritch R, Panda-Jonas S. Glaucoma. *Lancet*. Nov 11 2017;390(10108):2183-2193. doi:10.1016/S0140-6736(17)31469-1
4. Leske MC, Heijl A, Hussein M, et al. Factors for glaucoma progression and the effect of treatment: the early manifest glaucoma trial. *Arch Ophthalmol*. Jan 2003;121(1):48-56. doi:10.1001/archopht.121.1.48
5. You M, Rong R, Zeng Z, Xia X, Ji D. Transneuronal Degeneration in the Brain During Glaucoma. *Front Aging Neurosci*. 2021;13:643685. doi:10.3389/fnagi.2021.643685
6. Guymer C, Wood JP, Chidlow G, Casson RJ. Neuroprotection in glaucoma: recent advances and clinical translation. *Clin Exp Ophthalmol*. Jan 2019;47(1):88-105. doi:10.1111/ceo.13336

490 7. Zhang J, Li Z, Fan M, Jin W. Lipoxins in the Nervous System: Brighter Prospects for
491 Neuroprotection. *Front Pharmacol*. 2022;13:781889. doi:10.3389/fphar.2022.781889
492 8. Maderna P, Godson C. Lipoxins: resolutionary road. *Br J Pharmacol*. Oct
493 2009;158(4):947-59. doi:10.1111/j.1476-5381.2009.00386.x
494 9. Serhan CN. Pro-resolving lipid mediators are leads for resolution physiology. *Nature*. Jun
495 05 2014;510(7503):92-101. doi:10.1038/nature13479
496 10. Livne-Bar I, Wei J, Liu HH, et al. Astrocyte-derived lipoxins A4 and B4 promote
497 neuroprotection from acute and chronic injury. *The Journal of clinical investigation*. Dec 1
498 2017;127(12):4403-4414. doi:10.1172/jci77398
499 11. Serhan CN, Chiang N, Dalli J, Levy BD. Lipid mediators in the resolution of inflammation.
500 *Cold Spring Harb Perspect Biol*. Oct 30 2014;7(2):a016311. doi:10.1101/cshperspect.a016311
501 12. Wei J, Gronert K. The role of pro-resolving lipid mediators in ocular diseases. *Mol*
502 *Aspects Med*. Dec 2017;58:37-43. doi:10.1016/j.mam.2017.03.006
503 13. Flitter BA, Fang X, Matthay MA, Gronert K. The potential of lipid mediator networks as
504 ocular surface therapeutics and biomarkers. *Ocul Surf*. Jan 2021;19:104-114.
505 doi:10.1016/j.jtos.2020.04.008
506 14. Sofroniew MV. Molecular dissection of reactive astrogliosis and glial scar formation.
507 *Trends Neurosci*. Dec 2009;32(12):638-47. doi:10.1016/j.tins.2009.08.002
508 15. Colombo E, Farina C. Astrocytes: Key Regulators of Neuroinflammation. *Trends Immunol*.
509 Sep 2016;37(9):608-620. doi:10.1016/j.it.2016.06.006
510 16. Ding ZB, Song LJ, Wang Q, Kumar G, Yan YQ, Ma CG. Astrocytes: a double-edged sword in
511 neurodegenerative diseases. *Neural Regen Res*. Sep 2021;16(9):1702-1710. doi:10.4103/1673-
512 5374.306064
513 17. Liddelow SA, Guttenplan KA, Clarke LE, et al. Neurotoxic reactive astrocytes are induced
514 by activated microglia. *Nature*. Jan 26 2017;541(7638):481-487. doi:10.1038/nature21029
515 18. Zhang J, Li L, Huang H, et al. Silicone oil-induced ocular hypertension and glaucomatous
516 neurodegeneration in mouse. *Elife*. May 15 2019;8doi:10.7554/eLife.45881
517 19. Zhang J, Fang F, Li L, et al. A Reversible Silicon Oil-Induced Ocular Hypertension Model in
518 Mice. *J Vis Exp*. Nov 15 2019;(153)doi:10.3791/60409
519 20. Fang F, Zhang J, Zhuang P, et al. Chronic mild and acute severe glaucomatous
520 neurodegeneration derived from silicone oil-induced ocular hypertension. *Sci Rep*. Apr 27
521 2021;11(1):9052. doi:10.1038/s41598-021-88690-x
522 21. Guttenplan KA, Weigel MK, Prakash P, et al. Neurotoxic reactive astrocytes induce cell
523 death via saturated lipids. *Nature*. Nov 2021;599(7883):102-107. doi:10.1038/s41586-021-
524 03960-y
525 22. Liu HH, Flanagan JG. A Mouse Model of Chronic Ocular Hypertension Induced by
526 Circumlimbal Suture. *Invest Ophthalmol Vis Sci*. Jan 01 2017;58(1):353-361.
527 doi:10.1167/iovs.16-20576
528 23. Liu HH, Zhang L, Shi M, Chen L, Flanagan JG. Comparison of laser and circumlimbal
529 suture induced elevation of intraocular pressure in albino CD-1 mice. *PLoS One*.
530 2017;12(11):e0189094. doi:10.1371/journal.pone.0189094
531 24. Borgeson E, Johnson AM, Lee YS, et al. Lipoxin A4 Attenuates Obesity-Induced Adipose
532 Inflammation and Associated Liver and Kidney Disease. *Cell Metab*. Jul 07 2015;22(1):125-37.
533 doi:10.1016/j.cmet.2015.05.003

534 25. Gupta N, Yücel YH. Glaucoma as a neurodegenerative disease. *Curr Opin Ophthalmol*.
535 Mar 2007;18(2):110-4. doi:10.1097/ICU.0b013e3280895aea
536 26. Alqawlaq S, Flanagan JG, Sivak JM. All roads lead to glaucoma: Induced retinal injury
537 cascades contribute to a common neurodegenerative outcome. *Exp Eye Res*. Jun 2019;183:88-
538 97. doi:10.1016/j.exer.2018.11.005
539 27. Wei J, Gronert K. Eicosanoid and Specialized Proresolving Mediator Regulation of
540 Lymphoid Cells. *Trends Biochem Sci*. Mar 2019;44(3):214-225. doi:10.1016/j.tibs.2018.10.007
541 28. Pamplona FA, Vitória G, Sudo FK, et al. Age-linked suppression of lipoxin A4 associates
542 with cognitive deficits in mice and humans. *Transl Psychiatry*. Oct 10 2022;12(1):439.
543 doi:10.1038/s41398-022-02208-1
544 29. Siracusa R, Fusco R, Cuzzocrea S. Astrocytes: Role and Functions in Brain Pathologies.
545 *Front Pharmacol*. 2019;10:1114. doi:10.3389/fphar.2019.01114
546 30. Kim C, Livne-Bar I, Gronert K, Sivak JM. Fair-Weather Friends: Evidence of Lipoxin
547 Dysregulation in Neurodegeneration. *Mol Nutr Food Res*. Feb 2020;64(4):e1801076.
548 doi:10.1002/mnfr.201801076
549 31. Rådmark O, Werz O, Steinhilber D, Samuelsson B. 5-Lipoxygenase, a key enzyme for
550 leukotriene biosynthesis in health and disease. *Biochim Biophys Acta*. Apr 2015;1851(4):331-9.
551 doi:10.1016/j.bbalip.2014.08.012
552 32. Sapieha P, Stahl A, Chen J, et al. 5-Lipoxygenase metabolite 4-HDHA is a mediator of the
553 antiangiogenic effect of ω-3 polyunsaturated fatty acids. *Sci Transl Med*. Feb 09
554 2011;3(69):69ra12. doi:10.1126/scitranslmed.3001571
555 33. Wang SB, Hu KM, Seamon KJ, Mani V, Chen Y, Gronert K. Estrogen negatively regulates
556 epithelial wound healing and protective lipid mediator circuits in the cornea. *FASEB J*. Apr
557 2012;26(4):1506-16. doi:10.1096/fj.11-198036
558 34. Gao Y, Su J, Zhang Y, et al. Dietary DHA amplifies LXA. *Mucosal Immunol*. Nov
559 2018;11(6):1674-1683. doi:10.1038/s41385-018-0070-z
560 35. Bazan NG, Calandria JM, Serhan CN. Rescue and repair during photoreceptor cell
561 renewal mediated by docosahexaenoic acid-derived neuroprotectin D1. *J Lipid Res*. Aug
562 2010;51(8):2018-31. doi:10.1194/jlr.R001131
563 36. Gronert K. Lipoxins in the eye and their role in wound healing. *Prostaglandins Leukot*
564 *Essent Fatty Acids*. 2005;73(3-4):221-9. doi:10.1016/j.plefa.2005.05.009
565 37. Gronert K, Maheshwari N, Khan N, Hassan IR, Dunn M, Laniado Schwartzman M. A role
566 for the mouse 12/15-lipoxygenase pathway in promoting epithelial wound healing and host
567 defense. *J Biol Chem*. Apr 15 2005;280(15):15267-78. doi:10.1074/jbc.M410638200
568 38. Levy BD, Clish CB, Schmidt B, Gronert K, Serhan CN. Lipid mediator class switching during
569 acute inflammation: signals in resolution. *Nat Immunol*. Jul 2001;2(7):612-9. doi:10.1038/89759
570 39. Emerson MR, LeVine SM. Experimental allergic encephalomyelitis is exacerbated in mice
571 deficient for 12/15-lipoxygenase or 5-lipoxygenase. *Brain Res*. Sep 17 2004;1021(1):140-5.
572 doi:10.1016/j.brainres.2004.06.045
573 40. Ikonomovic MD, Abrahamson EE, Uz T, Manev H, Dekosky ST. Increased 5-lipoxygenase
574 immunoreactivity in the hippocampus of patients with Alzheimer's disease. *J Histochem*
575 *Cytochem*. Dec 2008;56(12):1065-73. doi:10.1369/jhc.2008.951855

576 41. Firuzi O, Zhuo J, Chinnici CM, Wisniewski T, Praticò D. 5-Lipoxygenase gene disruption
577 reduces amyloid-beta pathology in a mouse model of Alzheimer's disease. *FASEB J*. Apr
578 2008;22(4):1169-78. doi:10.1096/fj.07-9131.com
579 42. Chen F, Ghosh A, Lin J, et al. 5-lipoxygenase pathway and its downstream cysteinyl
580 leukotrienes as potential therapeutic targets for Alzheimer's disease. *Brain Behav Immun*. Aug
581 2020;88:844-855. doi:10.1016/j.bbi.2020.03.022
582 43. Lukiw WJ, Cui JG, Marcheselli VL, et al. A role for docosahexaenoic acid-derived
583 neuroprotectin D1 in neural cell survival and Alzheimer disease. *The Journal of clinical*
584 *investigation*. Oct 2005;115(10):2774-83. doi:10.1172/jci25420
585 44. Al-Shabrawey M, Zhang W, McDonald D. Diabetic retinopathy: mechanism, diagnosis,
586 prevention, and treatment. *Biomed Res Int*. 2015;2015:854593. doi:10.1155/2015/854593
587 45. van Leyen K, Klötzsch C, Harrer JU. Brain tumor imaging with transcranial sonography:
588 state of the art and review of the literature. *Ultraschall Med*. Dec 2011;32(6):572-81.
589 doi:10.1055/s-0031-1273443
590 46. Inman DM, Horner PJ. Reactive nonproliferative gliosis predominates in a chronic mouse
591 model of glaucoma. *Glia*. Jul 2007;55(9):942-53. doi:10.1002/glia.20516
592 47. Ben Haim L, Carrillo-de Sauvage MA, Ceyzériat K, Escartin C. Elusive roles for reactive
593 astrocytes in neurodegenerative diseases. *Front Cell Neurosci*. 2015;9:278.
594 doi:10.3389/fncel.2015.00278
595 48. Serhan CN, Hamberg M, Samuelsson B. Lipoxins: novel series of biologically active
596 compounds formed from arachidonic acid in human leukocytes. *Proc Natl Acad Sci U S A*. Sep
597 1984;81(17):5335-9. doi:10.1073/pnas.81.17.5335
598

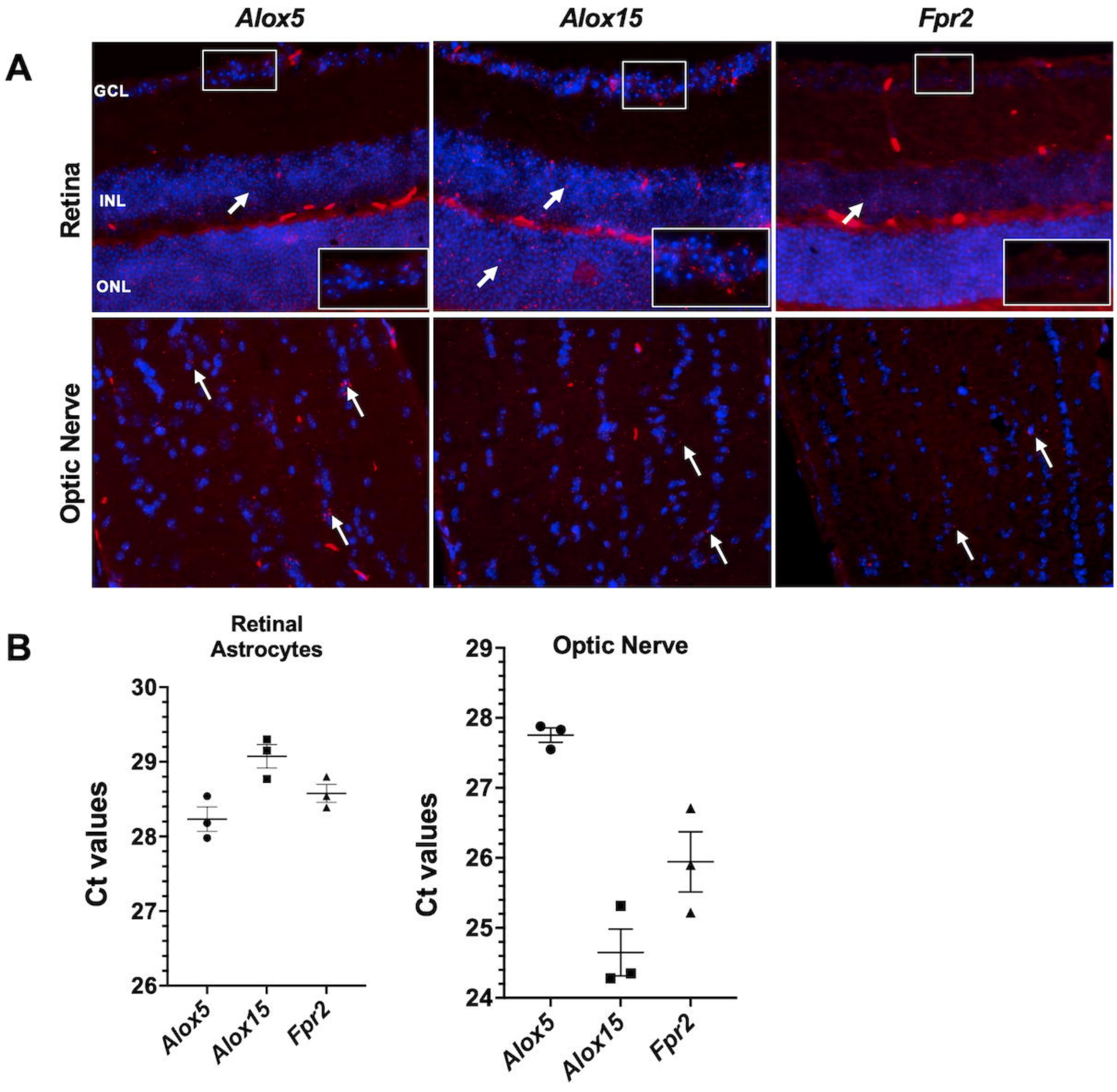
A
Alox5
Alox15
Fpr2
Retina
Optic Nerve
GCL
INL
ONL
B
Retinal Astrocytes
Optic Nerve
Ct values
30
29
28
27
26
25
24
Alox5
Alox15
Fpr2

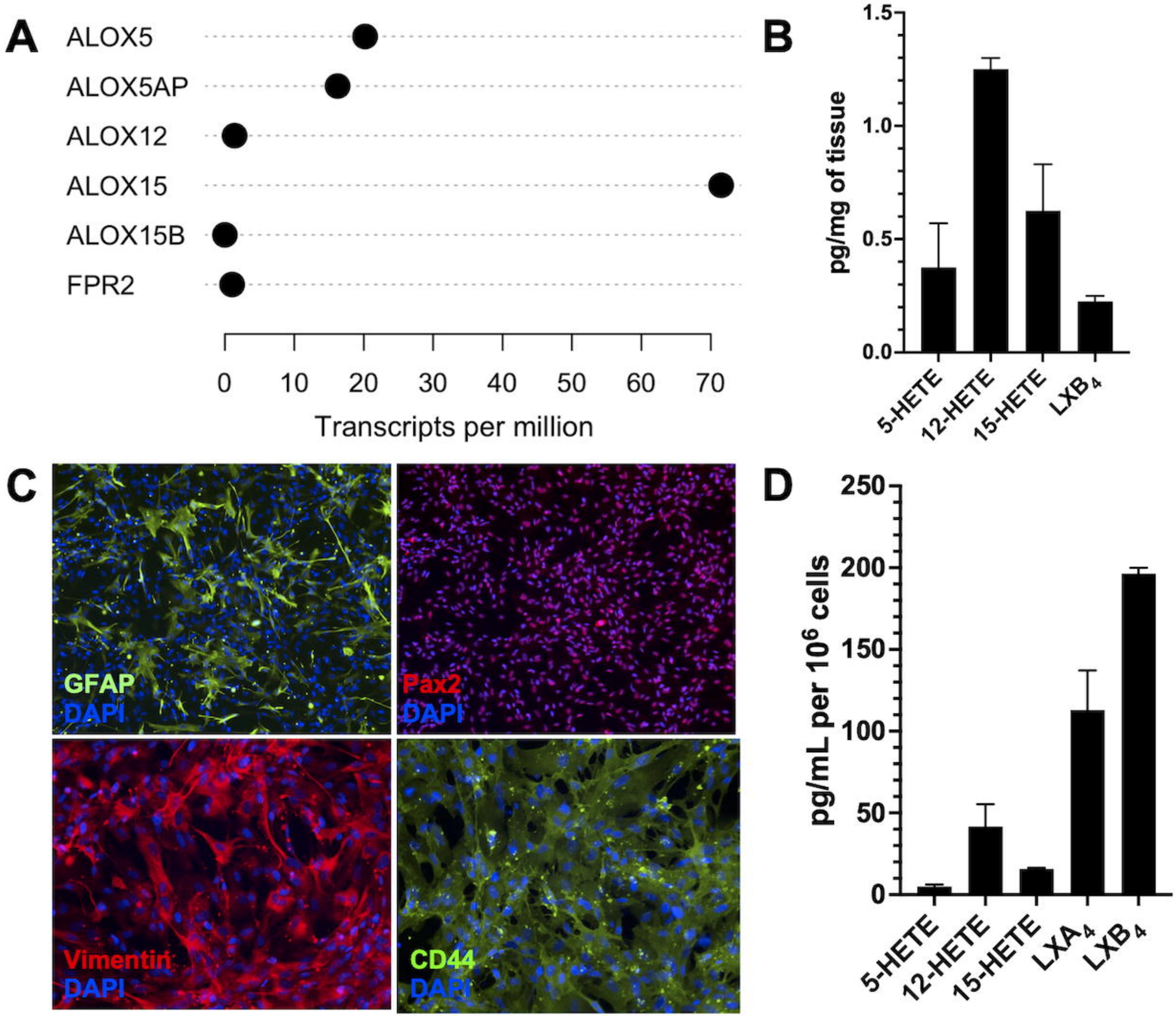
A
ALOX5
ALOX5AP
ALOX12
ALOX15
ALOX15B
FPR2
0
10
20
30
40
50
60
70
Transcripts per million
B
pg/mg of tissue
1.5
1.0
0.5
0.0
5-HETE
12-HETE
15-HETE
LXB4
C
GFAP
DAPI
Pax2
DAPI
Vimentin
DAPI
CD44
DAPI
D
pg/mL per 10^6 cells
250
200
150
100
50
0
5-HETE
12-HETE
15-HETE
LXA4
LXB4

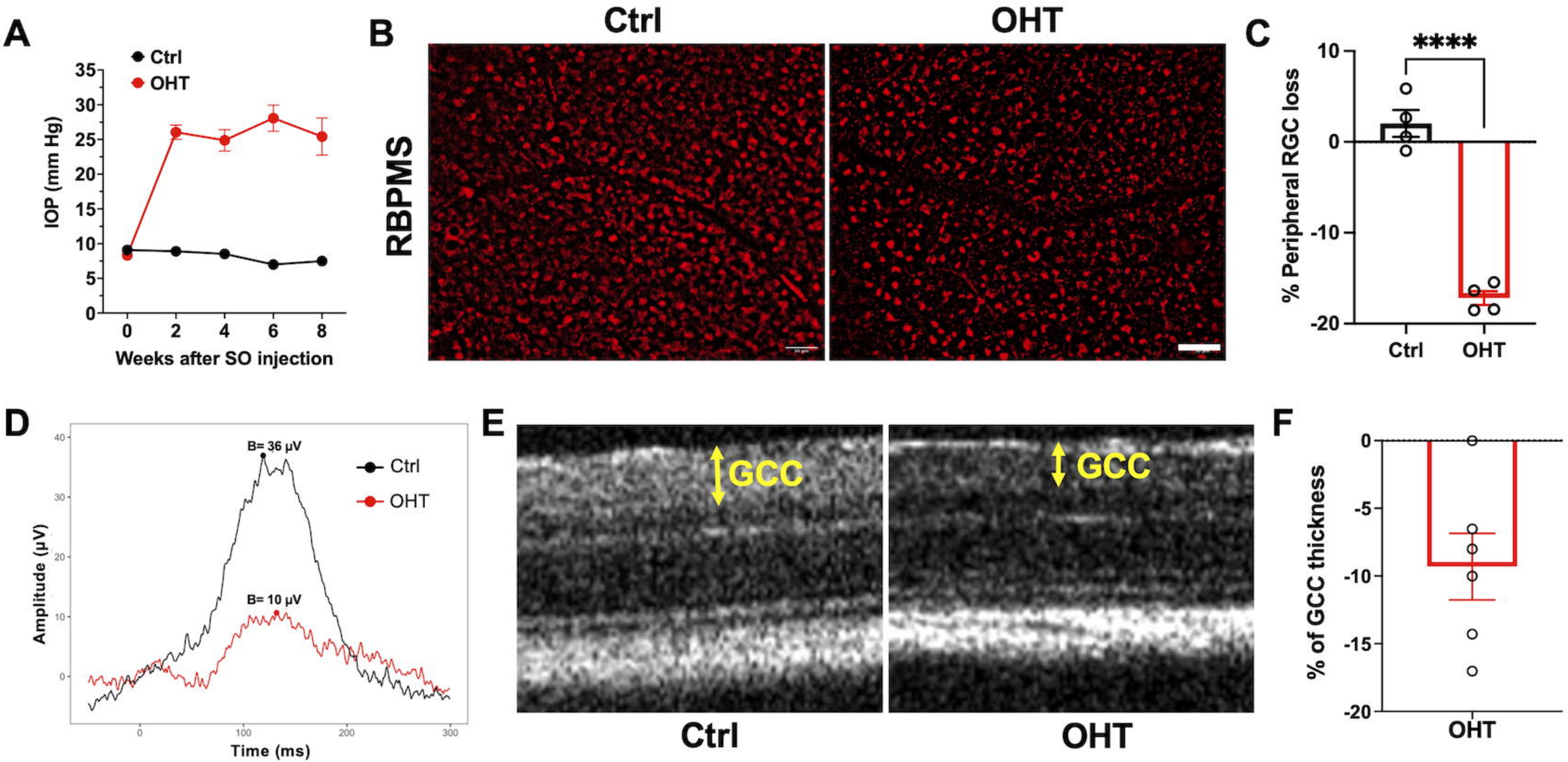
A
Ctrl
OHT
IOP (mm Hg)
35
30
25
20
15
10
5
0
0
2
4
6
8
Weeks after SO injection
B
Ctrl
OHT
RBPMS
C
****
% Peripheral RGC loss
10
0
-10
-20
Ctrl
OHT
D
B= 36 µV
B= 10 µV
Ctrl
OHT
Amplitude (µV)
40
30
20
10
0
0
100
200
300
Time (ms)
E
GCC
GCC
Ctrl
OHT
F
% of GCC thickness
0
-5
-10
-15
-20
OHT

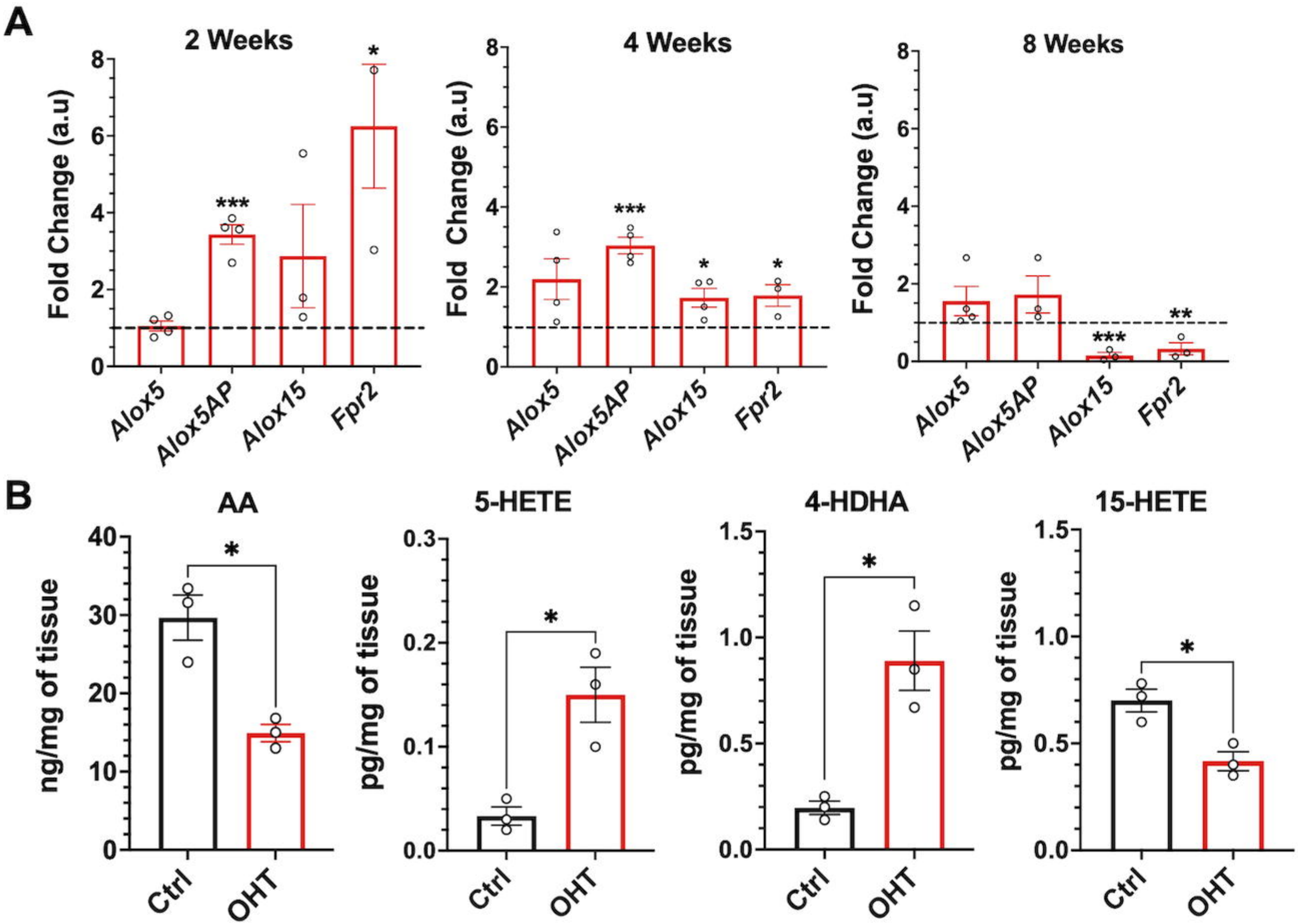
A
2 Weeks
4 Weeks
8 Weeks
Fold Change (a.u)
Alox5
Alox5AP
Alox15
Fpr2
B
AA
5-HETE
4-HDHA
15-HETE
ng/mg of tissue
pg/mg of tissue
Ctrl
OHT

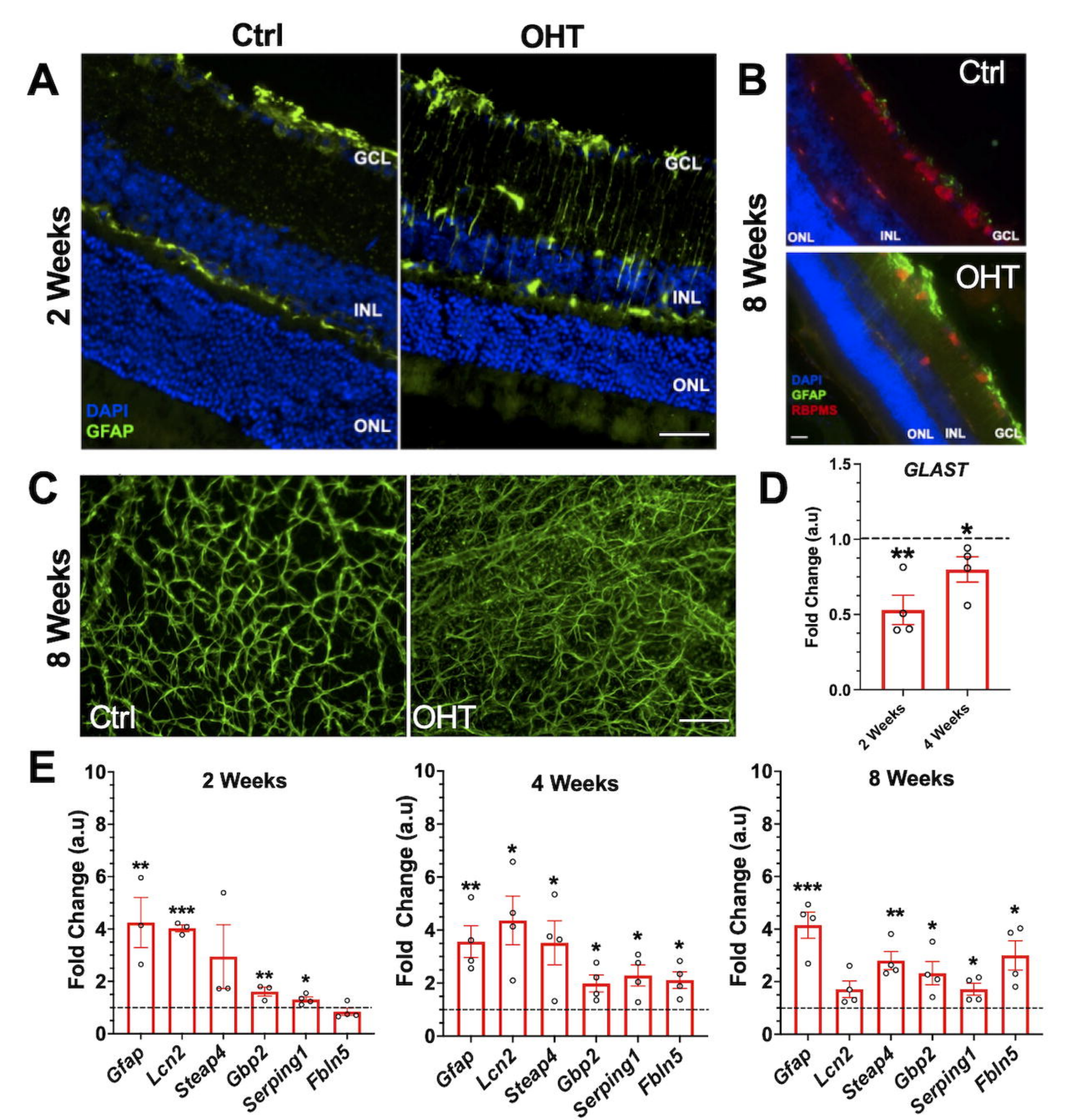
A
Ctrl
OHT
2 Weeks
GCL
INL
ONL
DAPI
GFAP
B
8 Weeks
Ctrl
OHT
ONL
INL
GCL
DAPI
GFAP
RBPMS
C
8 Weeks
Ctrl
OHT
D
GLAST
Fold Change (a.u)
1.5
1.0
0.5
0.0
**
*
2 Weeks
4 Weeks
E
2 Weeks
4 Weeks
8 Weeks
Fold Change (a.u)
10
8
6
4
2
0
Gfap
Lcn2
Steap4
Gbp2
Serping1
Fbln5

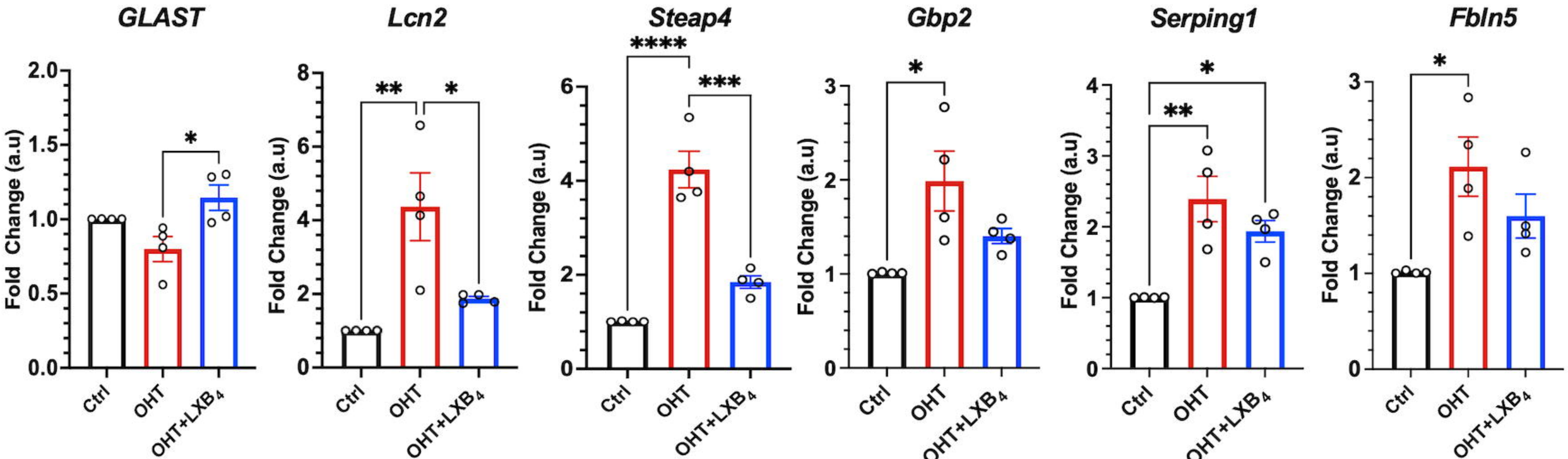
GLAST
Lcn2
Steap4
Gbp2
Serping1
Fbln5
Fold Change (a.u)
Ctrl
OHT
OHT+LXB4
*
**
***
****

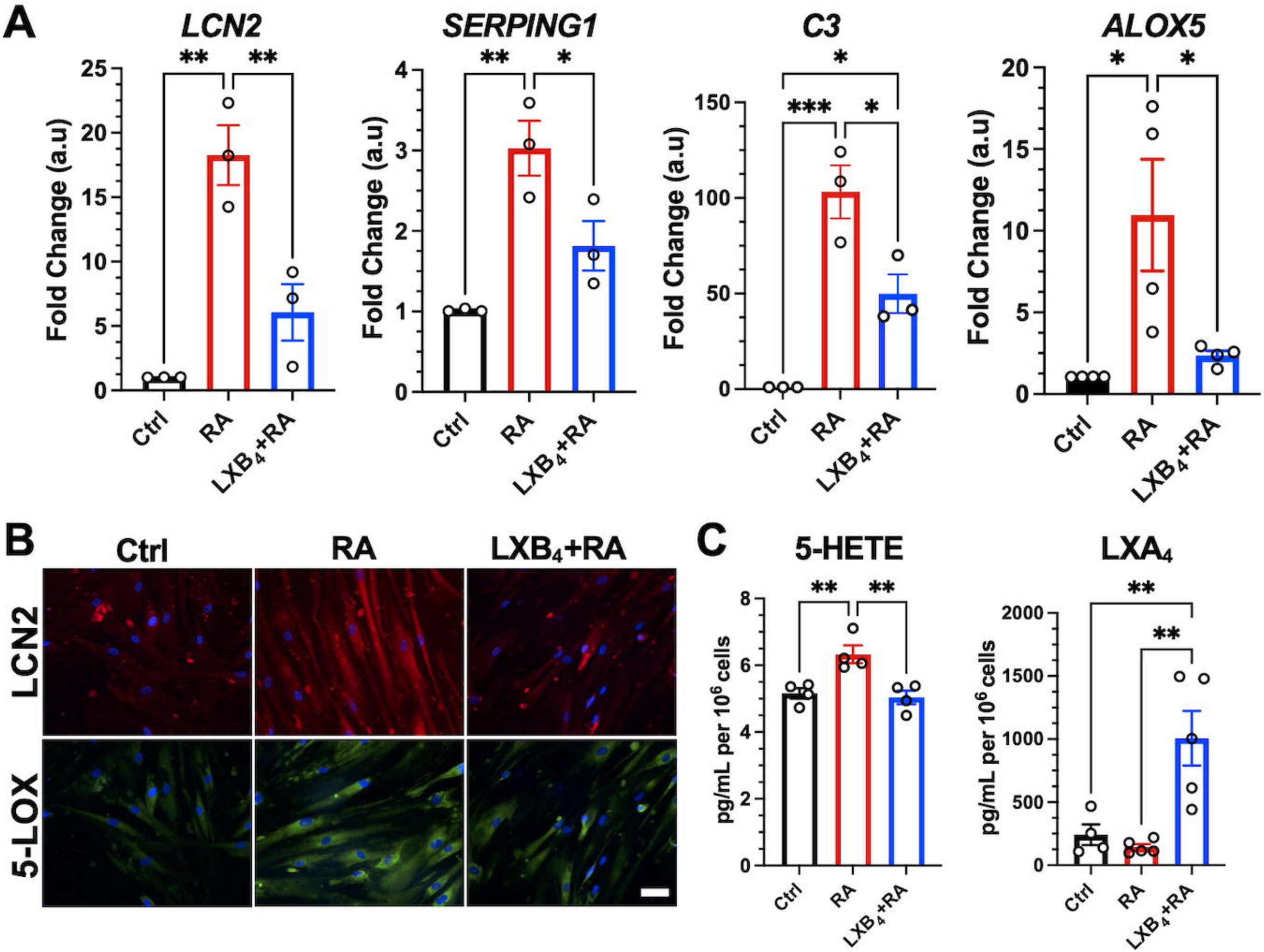
A
LCN2
SERPING1
C3
ALOX5
Fold Change (a.u)
Ctrl
RA
LXB4+RA
B
Ctrl
RA
LXB4+RA
LCN2
5-LOX
C
5-HETE
LXA4
pg/mL per 10^6 cells